Nuclear Instruments and Methods in Physics Research A 659 (2011) 403–410

Contents lists available at SciVerse ScienceDirect

Nuclear Instruments and Methods in Physics Research A

journal homepage: www.elsevier.com/locate/nima

Acceptance diagram calculations of the performance of neutron removal mirrors

J.R.D. Copley

NIST Center for Neutron Research, National Institute of Standards and Technology, Gaithersburg, MD 20899-6102, USA

ARTICLE INFO

Article history:
Received 7 April 2011
Received in revised form
2 August 2011
Accepted 3 August 2011
Available online 11 August 2011

Keywords:
Neutron removal mirror
Low energy neutron scattering
Neutron reflectivity
Acceptance diagrams
Ray-tracing calculations

ABSTRACT

We have used the method of acceptance diagrams to compute the performance of low energy neutron removal mirrors, or "deflectors", placed within a parallel neutron guide. Such devices are typically used to remove long wavelength neutrons from cold neutron beams. With appropriate coatings they may also be used as low energy neutron polarizers, ideally transmitting one spin state and reflecting the other spin state out of the beam. Within the small angle approximation, ignoring absorption, and representing reflectivities using unit step functions (either 0% or 100%, depending on the angle of incidence and the critical angle), the transmission probability reduces to a function of 3 ratios among 4 angles: the inclination angle of the deflector and the critical angles (which are proportional to neutron wavelength) of the upstream entrance guide, the deflector, and the guide within which the deflector is placed. The results of the acceptance diagram calculations, and of complementary ray-tracing calculations using realistic reflectivity profiles for the deflector, should benefit scientists and engineers involved in the design of neutron scattering instruments that potentially incorporate neutron deflectors.

Published by Elsevier B.V.

1. Introduction

From time to time the method of acceptance diagrams has been used to investigate the performance of various types of devices that transport neutrons into, and within, low energy neutron scattering instruments. Such devices include collimators, parallel guides and tapered guides [1–6] and, curved guides [7–9], as well as more specialized devices such as optical filters [10,11] and polarizing cavities [12]. Acceptance diagrams have also been used to study, inter alia, the focusing properties of curved neutron monochromators [13], the transmission properties of velocity selectors [14] and chopper systems [15–17], and a logarithmic spiral neutron guide [18]. Furthermore Cussen [19] has used acceptance diagrams to investigate a number of problems involving diffractometers, three-axis spectrometers, focusing monochromators, and novel beam elements. The basic idea of the acceptance diagram approach is to track *groups of neutrons*, represented as *areas* in an appropriate two-dimensional phase space. The alternative approach is to follow *individual neutrons*, each of which is represented as *a point* in phase space, using Monte Carlo ray-tracing techniques. Each approach has its advantages and disadvantages, depending on the problem at hand and on the purpose of the calculation. A recent advance, "neutron acceptance diagram shading" [20], alleviates some of the limitations of the traditional acceptance diagram approach.

The principal purpose of this paper is to evaluate the performance of neutron removal mirrors, such as the device illustrated in Fig. 1, using the method of acceptance diagrams: we shall use the term "deflector" to describe this type of device. Such devices have various uses. For example they are used to remove long wavelength neutrons from the polychromatic beams that supply time-of-flight reflectometers and small angle neutron scattering instruments. If coated with appropriately chosen materials they may also be used to polarize neutron beams.

Following some preliminary remarks we introduce the method of acceptance diagrams, illustrating its application to the simple case of a parallel guide. This also provides the opportunity to introduce terminology that is used in the discussion of the deflector system. Having worked through an example of a calculation for a deflector system, we present the results of calculations of the transmission probability for such systems as a function of three dimensionless ratios of angles. We briefly discuss additional ray-tracing calculations, including realistic reflectivity profiles for the deflector, and we conclude with brief remarks about polarizing cavity applications.

2. Preliminary remarks

We assume that angles of incidence are small so that the small angle approximation, $\tan\theta \approx \theta$, is justified. We also assume that reflecting surfaces reflect all neutrons incident at angles less than

E-mail address: john.copley@nist.gov

0168-9002/$ - see front matter Published by Elsevier B.V.
doi:10.1016/j.nima.2011.08.008

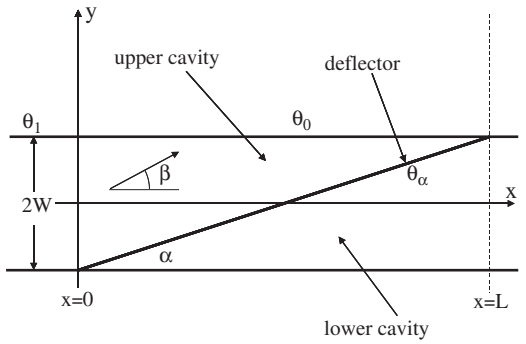

Fig. 1. Schematic of a long wavelength neutron removal mirror, or deflector. The origin of the (x,y) coordinate system is located at the mid-point of the entrance to the deflector. The angle that a neutron's trajectory makes with the axis of the system (the x axis) is β (positive as shown), and its distance from the x axis is y. The deflector section, between $x=0$ and $x=L$, is a guide section of width $2W$, with critical angle θ_0, within which is placed a reflecting surface (the deflector) with critical angle θ_α, inclined at angle α to the x axis. The deflector section is fed by a "long" parallel guide section with critical angle θ_1.

the critical angle for external reflection and that they transmit all neutrons incident at angles greater than the critical angle. It follows that we assume no absorption.

Our choice of coordinate system is illustrated in Fig. 1. The x axis is parallel to the axis of the guide and the y axis is normal. We only consider systems with a single transverse dimension y; allusions to "upper" and "lower" refer to larger and smaller values of the corresponding y coordinate. A neutron's position and direction are characterized, at any given value of x, by its transverse coordinate y and by the angle β that its direction makes with the x axis.

Critical angles θ may be expressed as $\theta=\lambda\gamma_0 m$, where λ is the wavelength, γ_0 is the critical angle per unit wavelength for natural nickel, which is ≈ 0.00173 rad/Å ($\approx 0.10\,^\circ$/Å), and m is the ratio of the critical angle of the reflecting surface to that of natural nickel. For example, the critical angle for 5 Å neutrons to be reflected by an "$m=3$" surface is ≈ 0.026 rad ($\approx 1.5^\circ$). (Note that 1 Å$=0.1$ nm.)

3. Parallel guide

In order to illustrate the acceptance diagram approach to calculations of the performance of neutron deflectors, we shall first consider the somewhat simpler arrangement illustrated in Fig. 2. A parallel guide (the "reference guide") is preceded by a fully illuminated "long" guide, i.e., a guide that is long enough that no neutron whose angle to the guide axis is greater than the critical angle can reach its exit.

3.1. An example

We start with a specific example in which the full width of both guides, $2W$, is 2 cm, and the length of the reference guide, L, is 160 cm. The critical angle for both guides is $\theta_0=0.0173$ rad (that of natural nickel for 10 Å neutrons), and there is an angular offset of $\eta=0.005$ rad, where the guide sections meet.

Neutrons entering the reference guide, at $x=0$, have $|y|\le W$ and $-0.0123\le\beta\le 0.0223$. Their distribution, assumed uniform, is represented by the *entrance acceptance diagram*, which is a single rectangle in (β,y) phase space bounded by the lines $\beta=0.005\pm 0.0173$ and $y=\pm W$ (Fig. 3a). Our task is to determine the *exit acceptance diagram*, which represents the (β,y) distribution at the exit of the guide. We do this by following groups of neutrons, represented by polygons in (β,y) space, as they proceed

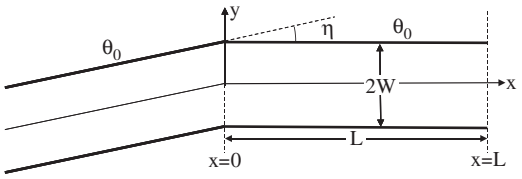

Fig. 2. A parallel guide section of length L, preceded by a "long" parallel guide section. The width of both guide sections is $2W$, and their common critical angle is θ_0. There is an angular offset η between the 2 sections.

through the guide. If a group escapes by transmission through a guide wall the corresponding polygon is retained as part of the final acceptance diagram. Groups encountering a surface will be reflected and/or transmitted. Multiple reflections may occur, and the process ends when all neutrons have escaped, either through the exit or through one of the guide walls.

If there were no guide each neutron's entrance coordinates, (β,y) at $x=0$, would transform to $(\beta,y+L\beta)$ at the exit, $x=L$. The corresponding acceptance diagram (Fig. 3a) is a parallelogram that we call the *empty system exit acceptance diagram*. Neutrons entering the reference guide section either reach the exit without encountering the guide (they are "conducted") or they strike one of the guide surfaces, in which case they are reflected or transmitted. The conducted neutrons, with $|y|<W$, are labeled M in Fig. 3(a) and C in the remaining panels of Fig. 3. The neutrons that strike the upper guide surface are those that would otherwise arrive at the exit plane with $y>W$. In other words they are represented by that part of the empty system diagram that is above the line $y=W$ (labeled U in Fig. 3a). Of these neutrons, those that are not reflected and therefore escape have $\beta>\theta_0$; they correspond to the part of the empty system diagram that is above the line $y=W$, and to the right of the line $\beta=\theta_0$ (labeled A in Fig. 3b). Those that are reflected, having $0<\beta\le\theta_0$, lie to the left of the line $\beta=\theta_0$. Reflection at the upper guide surface transforms a neutron's coordinates at the exit, assuming free propagation following reflection, from (β,y) to $(-\beta,2W-y)$. In the acceptance diagram this corresponds to a 180° rotation about the mid-point, $(0,W)$ (Fig. 3b, polygon G). The neutrons that strike the lower guide surface are similarly treated; the polygon obtained following a 180° rotation of the original polygon (labeled L) about the mid-point, $(0,-W)$, represents neutrons once reflected by the lower surface (Fig. 3c, polygon K). No neutrons are transmitted through the lower surface.

We need not concern ourselves further with the neutrons that were conducted or escaped by transmission (polygons C and A, respectively). The only neutrons that need to be considered further are those represented by the polygons in Fig. 3(c) labeled G and K. Since the latter polygon lies between the lines $y=\pm W$, the corresponding group of neutrons reaches the exit without additional encounters with the guide (polygon KC in Fig. 3d). On the other hand the part of the polygon labeled G with $y<-W$ represents neutrons that strike the lower guide wall and are reflected a second time, since $\beta>-\theta_0$. Thus polygon G in Fig. 3(c) is broken into polygons labeled GC and GKC in Fig. 3(d). The conducted fraction is 85.5%, including 36.1% conducted to the exit, 46.8% once reflected, and 2.7% twice reflected. The remaining 14.5% escape through the upper guide wall.

3.2. General remarks

At any stage in the development of the final acceptance diagram, each polygon has an associated *history* that lists, in chronological order, what had previously happened at each encounter with a reflecting surface. Fig. 3(d) shows several examples of polygon histories. The current situation associated

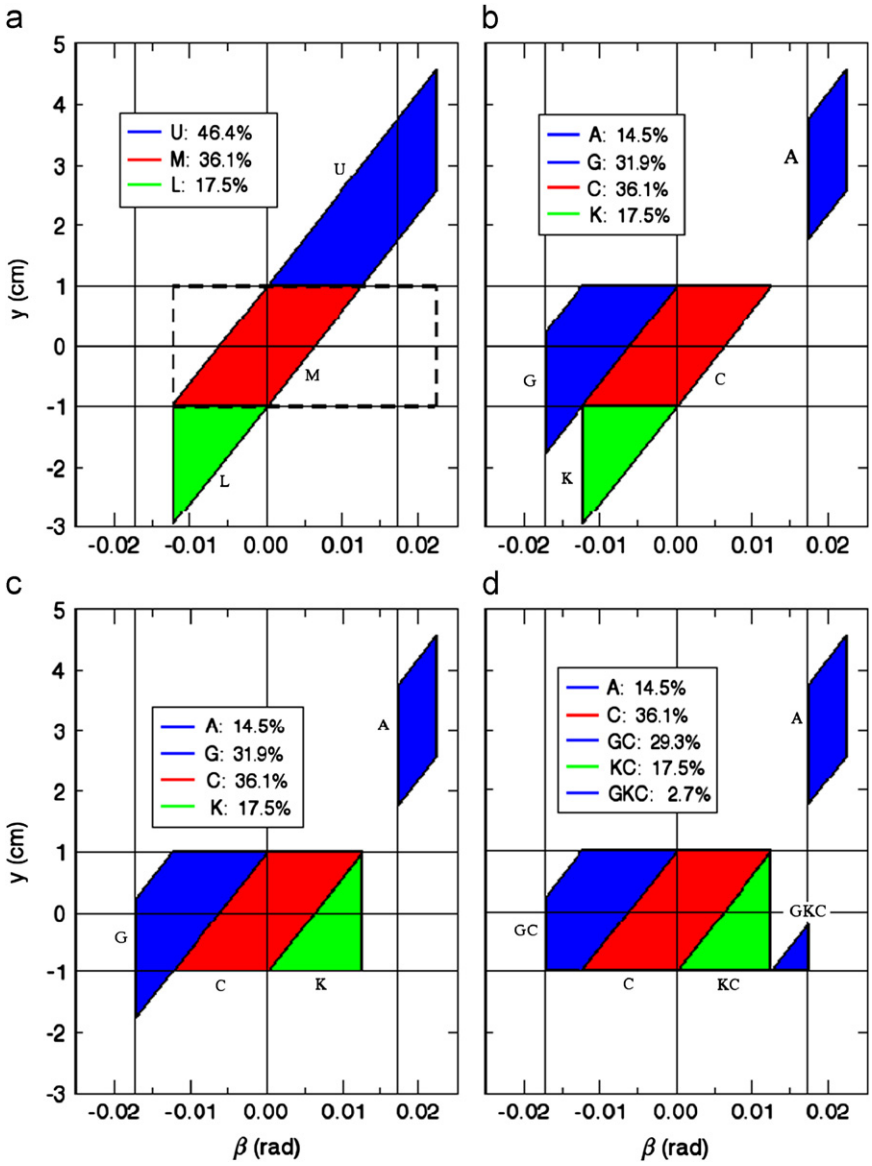

Fig. 3. Acceptance diagrams for the guide system shown in Fig. 2, with $2W=2$ cm, $L=160$ cm, $\theta_0=0.0173$ rad, and $\eta=0.005$ rad. Horizontal lines are drawn at $y=0$ and $y=\pm W$, and vertical lines are drawn at $\beta=0$ and $\beta=\pm\theta_0$. In panel (a) the dashed rectangle is the entrance diagram and the multicolored parallelogram is the empty system exit diagram. The blue and green polygons, labeled U and L, represent neutrons that strike the upper and lower guide surfaces, respectively; the red polygon, labeled M, represents neutrons destined to exit the reference guide without hitting either guide surface (outcome C). In panel (b) the blue polygon has been separated into a portion that is rotated about the point $(0,W)$, representing neutrons reflected by the upper surface (label G), and a portion that remains, representing neutrons transmitted through the upper surface (label A). In panel (c) the green triangle, labeled K, has been rotated about the point $(0,-W)$, representing neutrons reflected by the lower surface, and in (d) the blue triangle, also obtained by rotation about the point $(0,\ -W)$ and labeled GKC, represents neutrons reflected off the upper and lower surfaces successively. Each polygon has an associated history and relative intensity. Due to rounding, intensities do not necessarily add up to unity. (For interpretation of the references to color in this figure legend, the reader is referred to the web version of this article).

with a polygon is called its *state*. For the general case of a parallel guide we define (for convenience) the incoming state I, which is immediately broken into three possible states (Fig. 4a). Those headed for the exit without encountering the guide are in state M. Those destined to strike the upper and lower guide surfaces are in states U and L, respectively. Possible future states, or *outcomes*, for neutrons in state U, are reflection (state G) and escape by transmission (state A). By the same token possible outcomes for neutrons in state L are reflection (state K) and escape by transmission (state E). (In the example discussed above there are no neutrons in state E.) States and outcomes are illustrated in Fig. 4(a) whereas relationships among the states are shown in Fig. 4(b). The only outcome for neutrons in state M is state C. Subsequent possible outcomes for neutrons reflected by the upper (lower) guide surfaces are K and C (G and C). (If the upper and lower guide surfaces had different critical angles, either outcome A or outcome E, but not both, would be a third possibility following reflection.)

4. Deflector system

The deflector system, illustrated in Fig. 1, comprises a section of guide within which is placed a reflecting surface (the deflector) that is inclined at an angle α to the x axis. The length of the system is L and its width is $2W=\alpha L$ (within the small angle approximation). The critical angles of the guide and of the deflector are θ_0 and θ_α, respectively. The system is fed by a fully illuminated "long" guide (defined in Section 3), with critical angle θ_1 and width 2W.

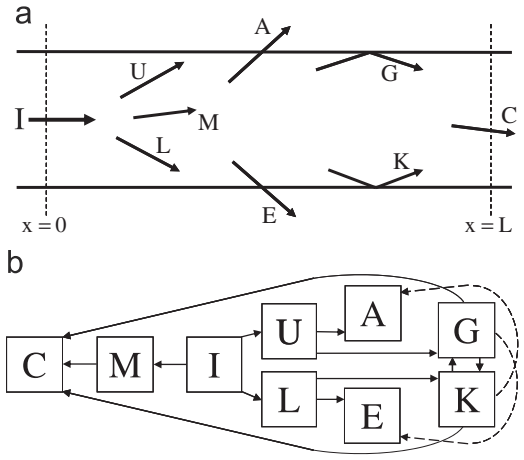

Fig. 4. (a) Possible states and outcomes for a parallel guide. For example neutrons in state U are destined to strike the guide's upper surface, and possible outcomes are reflection (G) and escape by transmission (A); (b) a relationship diagram representing possible states and outcomes for a parallel guide. The dashed lines, from G to E and from K to A, point to outcomes that only exist (one or the other but not both) when the guide surfaces have different critical angles.

4.1. An example

To illustrate the acceptance diagram approach we shall first consider a specific example. The width and length of the deflector section, $2W$ and L, are 2 cm and 115.61 cm, respectively, such that $\alpha=2W/L=0.0173$ rad. The critical angles of the various surfaces are $\theta_1=0.0173$ rad, $\theta_0=\theta_1/2$, and $\theta_\alpha=\theta_1$.

The entrance acceptance diagram is a rectangle bounded by the lines $y=\pm W$ and $\beta=\pm\theta_1$, and the corresponding empty system exit acceptance diagram (introduced in Section 3) is a parallelogram bounded by the lines $y=\pm W+L\beta$ and $\beta=\pm\theta_1$ (Fig. 5a). Neutrons entering the deflector will either strike the upper guide surface from below or the deflector surface from above. Those that, in the absence of reflecting surfaces, would arrive at the exit plane with $y>W$, in actual fact strike the upper guide surface (state U). Conversely those that, in the absence of reflecting surfaces, would arrive at the exit with $y<W$, in actual fact strike the deflector surface from above (state L). Thus the polygons above and below the line $y=W$ in the empty system acceptance diagram represent neutrons in states U and L, respectively (Fig. 5a).

Neutrons in state U with $\beta>\theta_0$ escape through the upper guide surface. They are represented by the polygon labeled A in Fig. 5(b). The remaining neutrons in state U are reflected off the upper guide surface (polygon G in Fig. 5b, obtained by 180° rotation about (0,W)) and approach the deflector from above. They are all transmitted and their history becomes GS (see also Fig. 6a).

The neutrons in state L that are reflected off the upper deflector surface have $\beta>-\theta_\alpha+\alpha$, i.e., $\beta>0$. They are represented by the polygon labeled H (Fig. 5b), and the reflection is represented by a 180° rotation about the point (α,W) (Fig. 5c). These neutrons subsequently encounter the upper guide surface from below and they all escape. Their history is HA (Fig. 5d).

The neutrons that entered the deflector section and were transmitted through the deflector into the lower cavity (those in state S), suffer three possible outcomes. The first two outcomes, both of which take place in our example, are transmission through the lower guide surface (outcome E, history SE), and reflection by the lower guide surface (outcome K, history SK). The other possible outcome is conduction through the exit of the deflector section, outcome C (history SC).

There are two groups of neutrons that have not yet escaped. Their histories are GS and SK. The GS neutrons are handled as previously described. They escape through the exit with history GSC (Fig. 5d). The neutrons whose history is SK have three possible outcomes: C, J, and T (Fig. 6a). In the present example they all escape through the exit with history SKC (Fig. 5d).

This completes the analysis of our example: 7/16 (43.75%) of the neutrons escape through the top surface (histories A and HA), 3/16 (18.75%) through the bottom surface (history SE), and the remaining 3/8 (37.5%) exit the deflector section (histories SC, GSC, and SKC).

4.2. General method

Neutrons entering the deflector (in initial state I) will either strike the upper guide surface from below or the deflector surface from above. For convenience we call these situations U and L, respectively. In either case the neutrons may in general be reflected or transmitted. Thus there are four possible outcomes (A, G, H, and S) following the initial encounter with a surface (Fig. 6a and b). The neutrons that strike the upper guide surface are those that would otherwise arrive at the exit plane with $y>W$. Of these neutrons those that are not reflected and therefore escape (outcome A) have $\beta>\theta_0$, whereas those that are reflected (outcome G) have $\beta\le\theta_0$. This type of reflection, at the upper guide surface, transforms a neutron's coordinates at the exit, in the absence of further encounters, from (β,y) to ($-\beta$,$2W-y$). In the acceptance diagram this corresponds to a 180° rotation about the mid-point (0,W).

Consider now the neutrons that strike the inclined deflector surface from above (state L, Fig. 6a). Those that are not reflected and pass into the lower cavity (outcome S) have $\beta<-\theta_\alpha+\alpha$, whereas those that are reflected, remaining in the upper cavity (outcome H), have $\beta>-\theta_\alpha+\alpha$. Reflection at the deflector surface transforms a neutron's exit coordinates (as before assuming no further encounters) from (β,y) to ($2\alpha-\beta$,$2W-y$). In the acceptance diagram this corresponds to a 180° rotation about the mid-point (α,W).

Additional interactions with the guide and deflector surfaces are handled using a "level-order traversal algorithm"[21] that follows each remaining group of neutrons to its next encounter and continues in this fashion until all neutrons have escaped, either through one of the guide walls or through the exit.

All told there are 12 possible states, listed in Table 1 and illustrated in Fig. 6(a). They include 3 possible escape routes (A, C, and E), 4 states that follow reflection (G, H, J, and K), and 2 states that follow transmission through the deflector plate (S and T), plus the initial states I, U, and L. Also listed in Table 1, for each of the 9 non-escape states, are possible outcomes. Relationships among the states are depicted in Fig. 6(b), and additional procedural information may be found in the Appendix.

5. Results

Given the assumption of perfect reflectivity up to the critical angle, and zero reflectivity (as well as zero absorption) at higher angles, the behavior of any given neutron deflector arrangement depends on 4 angles: the critical angles θ_0, θ_1, and θ_α, and the inclination angle α. Within the small angle approximation it reduces to a function of 3 ratios: $\kappa=\theta_0/\theta_1=m_0/m_1$, $\rho=\theta_\alpha/\theta_1=m_\alpha/m_1$, and $\chi=\theta_1/\alpha=\lambda\gamma_0 m_1/\alpha$. In what follows we shall discuss the transmission probability, $T(\kappa,\rho,\chi)$, which is obtained as the ratio of two acceptance diagram areas. The denominator is simply $4\theta_1 W$, which is the area of the entrance diagram, representing those neutrons that enter the deflector section at $x=0$.

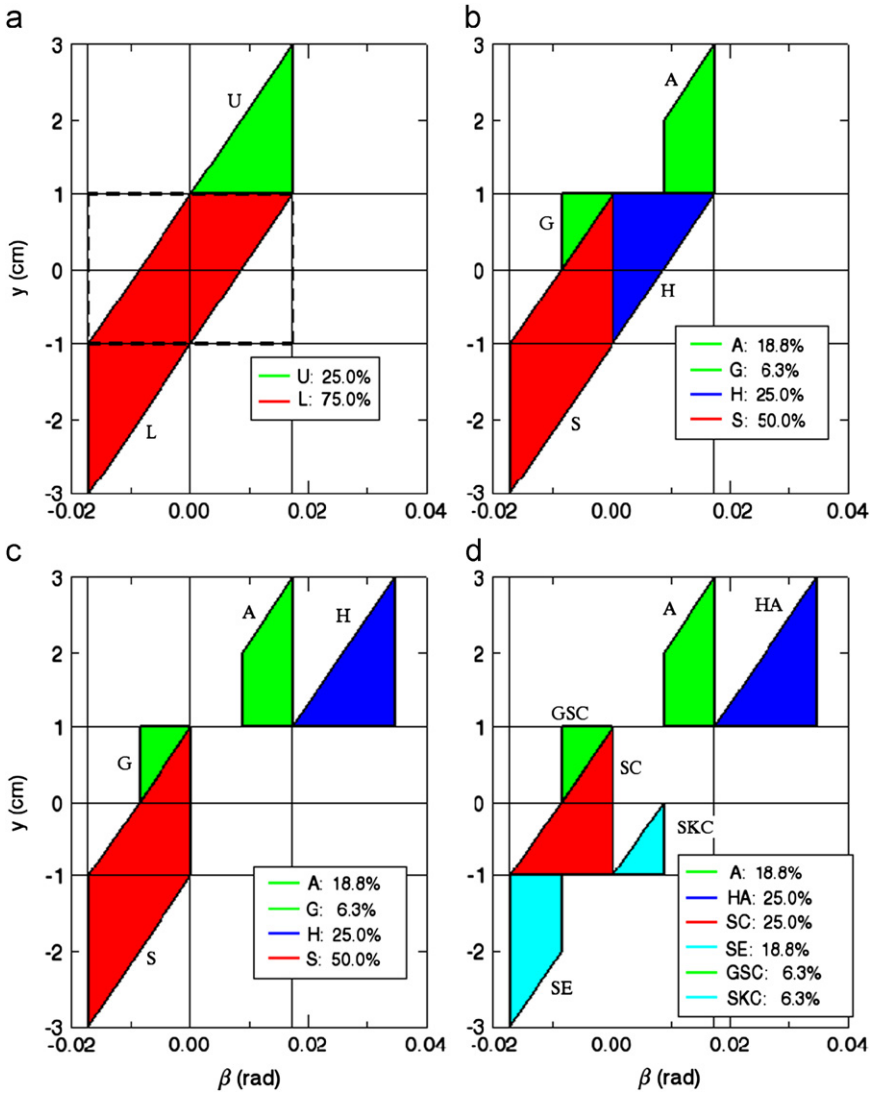

Fig. 5. Acceptance diagrams for the deflector system illustrated in Fig. 1; $2W=2$ cm and $L=115.61$ cm, so $\alpha=0.0173$ rad. Critical angles are $\theta_1=0.0173$ rad, $\theta_0=\theta_1/2$, and $\theta_\alpha=\theta_1$. Horizontal lines are drawn at $y=0$ and $y=\pm W$, and vertical lines are drawn at $\beta=0$ and $\beta=\pm\theta_1$. In panel (a) the dashed rectangle is the entrance diagram and the multicolored parallelogram is the empty system exit diagram. The green and red polygons, labeled U and L, represent neutrons that strike the upper guide surface and the deflector from above, respectively. In panel (b) the green polygon (U) has been separated into (i) a portion that has been rotated about the point (0,W), representing neutrons reflected by the upper guide surface (state G), and (ii) a portion that remains, representing neutrons transmitted through the upper guide surface (state A). Similarly the red polygon, labeled L in panel (a), has been separated into (i) a blue triangle labeled H (panel b) that has been rotated in panel (c) about the point (α,W), representing neutrons reflected by the upper surface of the deflector, and (ii) a portion that remains (labeled S), representing neutrons transmitted through the deflector. In panel (d) the polygon labeled S has been separated into 3 portions: (i) the triangle labeled SC, representing neutrons conducted to the exit, (ii) the polygon labeled SE, representing neutrons that strike the lower guide surface and escape, and (iii) the triangle labeled SKC, representing neutrons that are reflected by the lower surface and then leave through the exit. Each polygon has an associated history and relative intensity. Due to rounding, intensities do not necessarily add up to unity. In the language of Section 5, the dimensionless parameters for this arrangement are $\kappa=0.5$, $\rho=1$, and $\chi=1$. (For interpretation of the references to color in this figure legend, the reader is referred to the web version of this article)

The numerator is the sum of the areas of all polygons with final outcome C, representing any and all neutrons that pass through the exit (with $|y|<W$ at $x=L$).

Fig. 7 shows the calculated transmission probability T for selected values of ρ with $\kappa=1$, which represents the situation where a deflector plate is inserted into a continuous guide. The $\rho=0.5$ and $\rho=2$ curves are identical to Mezei's curves for the polarizing cavity (the solid lines in Fig. 3 of Ref. [12]). The acceptance diagrams for $\chi=0.75$, with $\rho=0.5$ and $\rho=2$, agree with those shown in Fig. 10 of Ref. [3]. The abscissa χ is proportional to the wavelength. Neutrons with $\chi\le 1/(\rho+1)$, i.e., $\lambda\le(\alpha/\gamma_0 m_1(\rho+1))$, are 100% transmitted whereas when $\rho>1$ and $\chi\ge 1/(\rho-1)$, i.e., $\lambda\ge(\alpha/\gamma_0 m_1(\rho-1))$, no neutrons are transmitted. These inequalities may be obtained by considering the degree of overlap between the range of angles β for neutrons entering the deflector system and the range of angles reflected by the deflector. Evidently ρ must be large if an abrupt change in T with wavelength is desired, as is often the case.

Fig. 8 shows $T(\kappa,\rho,\chi)$ for various choices of ρ, this time with $\kappa=0$, which corresponds to the situation where the deflector is installed in a guide cut, rather than within a section of guide. The curve for $\rho=0$, which we shall call the bare guide cut curve, represents the case where there is no deflector plate, so that there is nothing but a simple guide cut. In this case $T=1-\chi/2$ for $0\le\chi\le 1$ and $T=1/2\chi$ for $1\le\chi$. The curve for any choice of $\rho>0$ appears to meet the bare guide cut curve at $\chi=1/(\rho+1)$.

A comparison of results for $\kappa=0$, in which case the deflector is in a guide cut, and $\kappa=1$, in which case the deflector is within a continuous guide, for two values of ρ, is shown in Fig. 9. In a sense the change in transmission with wavelength is somewhat sharper when $\kappa=0$, but in this case the transmission is also reduced at short wavelengths such that $\chi<1/(\rho+1)$.

Fig. 10 shows results for $\kappa=1.5$. In this case the behavior of T with χ appears to be the same as for $\kappa=1$ at the larger values of ρ, but it is very different at intermediate and small values of ρ. In large part this is due to contributions from neutrons that exit the deflector section at angles greater than the critical angle of the entrance guide, θ_1. The dashed lines show transmission probabilities computed excluding all neutrons with $|\beta|>\theta_1$. There is no obvious use for a deflector system with $\kappa>1$.

6. Discussion

The acceptance diagram approach, as described in this paper, is exact, but it has its limitations. For example reflectivities are generally described by unit step functions such that the reflectivity at any given angle is either 0% or 100%. To a large extent these types of limitations may be removed using the acceptance diagram shading algorithm [20]. The alternative approach, that of ray-tracing (otherwise known as "Monte-Carlo"), continues to enjoy widespread popularity. We have performed a number of ray-tracing calculations for comparison with the "exact" results obtained using acceptance diagrams, and without exception the two methods yield results that are identical within statistics.

We have also used ray-tracing to investigate the effect of using a realistic reflectivity profile for the deflector plate. Fig. 11 shows ray-tracing and exact results for 2 arrangements that result in the same lower cutoff, at 18 Å. The parameters of the calculations are given in the figure caption. The decrease in T with increasing λ is clearly much faster when ρ and α are increased but this observation is largely academic since supermirror coatings with large values of m have significantly reduced reflectivity, especially at angles comparable with the critical angle. The results of calculations using realistic reflectivity profiles (C. Schanzer and P. Böni, private communication, 2011) show that very significant changes may take place when such profiles are included, especially when ρ is large (Fig. 11).

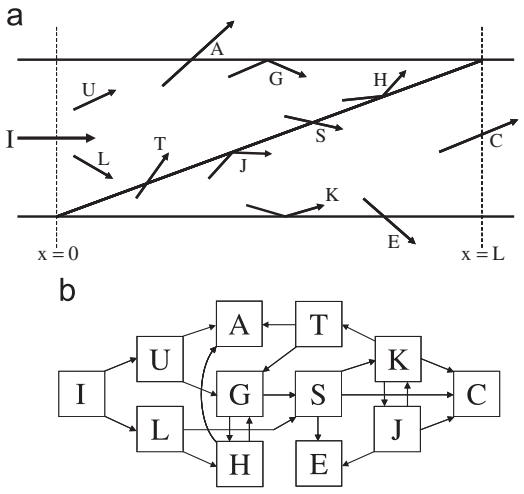

Fig. 6. (a) Possible states and outcomes for a deflector system. For example neutrons in state L (and in state G) approach the upper surface of the deflector, and possible outcomes are reflection (H) and transmission (S). Subsequent outcomes for neutrons in state S are reflection (K), transmission at the lower guide surface (E), and conduction through the guide exit (C).;(b) The corresponding relationship diagram. Final outcomes are A, E, and C.

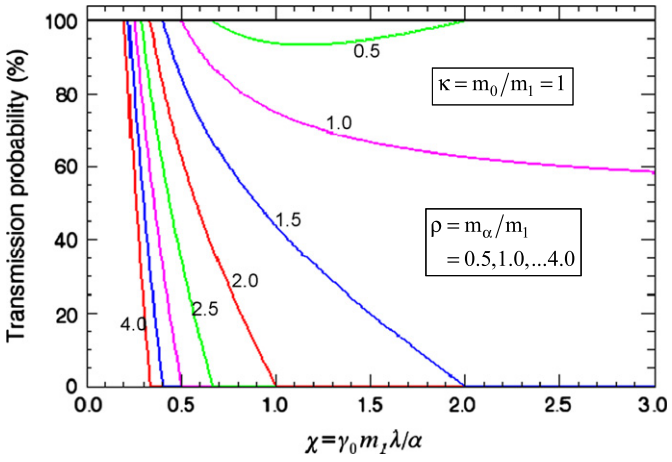

Fig. 7. $T(\kappa,\rho,\chi)$ for $\kappa=1$ and values of ρ from 0.5 to 4.0 in steps of 0.5.

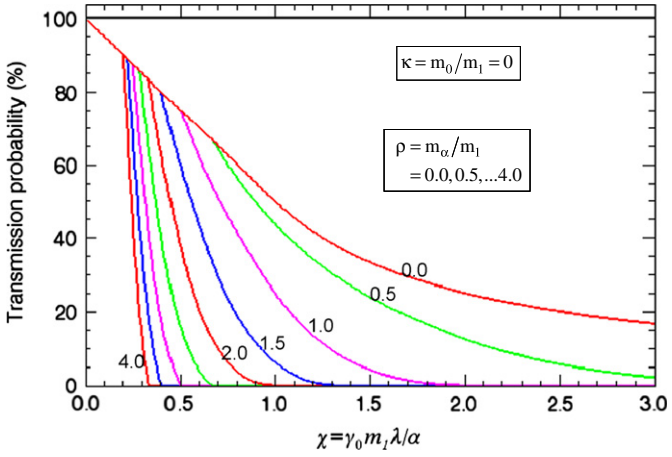

Fig. 8. $T(\kappa,\rho,\chi)$ for $\kappa=0$ and values of ρ from 0.0 to 4.0 in steps of 0.5.

Table 1
Possible states and outcomes for a single deflector.

State	Description	Outcomes
A	Escaped by transmission through upper guide (with $\beta>\theta_0$)	–
C	Escaped through exit	–
E	Escaped by transmission through lower guide (with $\beta<-\theta_0$)	–
G	Reflected by upper guide, approaching deflector	H,S
H	Reflected by deflector's upper surface, approaching upper guide	A,G
I	Entered deflector section	L,U
J	Reflected by deflector's lower surface, approaching lower guide or exit	C,E,K
K	Reflected by lower guide, approaching deflector or exit	C,J,T
L	Entered deflector section, approaching lower guide	H,S
S	Transmitted through deflector, approaching lower guide or exit	C,E,K
T	Transmitted through deflector, approaching upper guide	A,G
U	Entered deflector section, approaching upper guide	A,G

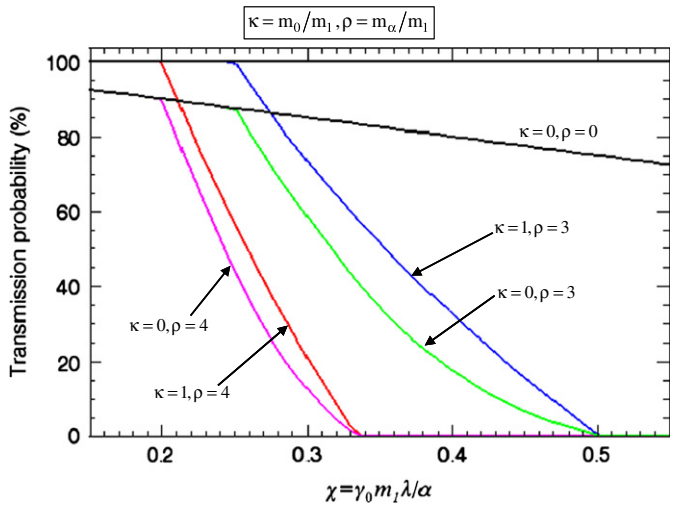

Fig. 9. $T(\kappa,\rho,\chi)$ for $\kappa=0$ and 1, $\rho=3$ and 4. Also shown is $T(\kappa,\rho,\chi)$ for $\kappa=0$, $\rho=0$.

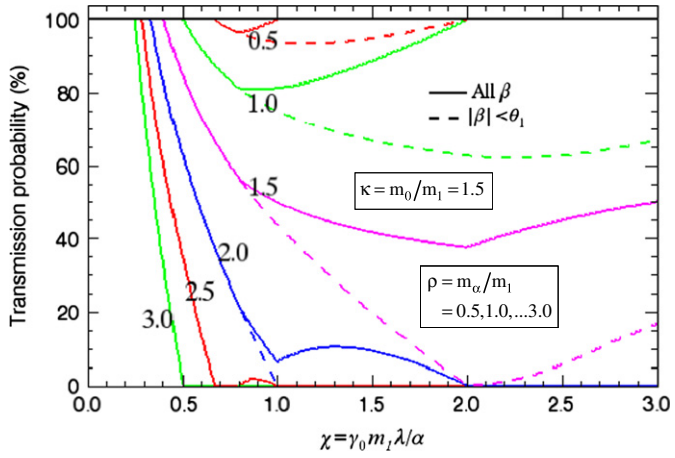

Fig. 10. Solid lines show $T(\kappa,\rho,\chi)$ for $\kappa=1.5$ and values of ρ from 0.5 to 3.0 in steps of 0.5. Dashed lines show the contribution to T from neutrons with $|\beta|<\theta_1$.

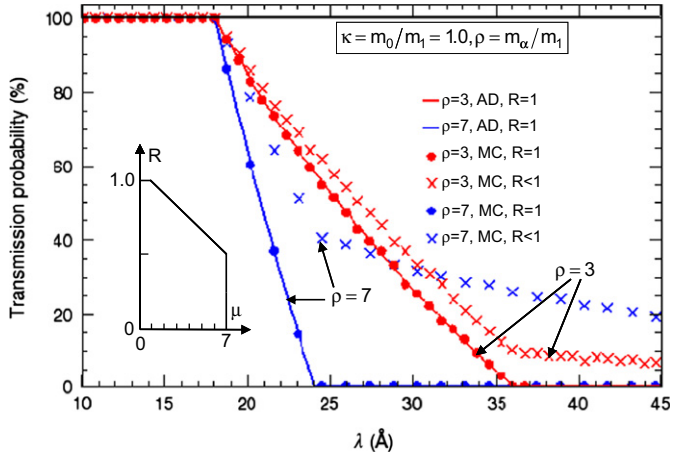

Fig. 11. Results of exact (AD) and ray-tracing (MC) calculations for two arrangements that result in the same lower cutoff, at 18 Å. In both cases $m_1=m_0=1$, i.e., $\kappa=1$. The exact calculations, shown as lines, are for $\alpha=7.2'$ with $m_\alpha=3$ (labeled $\rho=3$), and for $\alpha=14.4'$ with $m_\alpha=7$ (labeled $\rho=7$). The same parameters were used for the MC calculations labeled "$R=1$", shown as filled circles. These calculations assume stepwise reflectivity, i.e., $R=1$ when $\mu\le m_\alpha$ and $R=0$ when $\mu>m_\alpha$, where $\mu=\theta/\gamma_0\lambda$. Additional MC calculations, using realistic reflectivity profiles, are labeled "$R<1$" and shown as crosses. For these calculations the following reflectivity profile, illustrated in the figure for $m_\alpha=7$, was assumed: $R=1$ when $\mu\le 1$; $R=1+(\mu-1)c$ with $c=-0.0833$ when $1<\mu\le m_\alpha$; and $R=0$ when $\mu>m_\alpha$.

The acceptance diagram approach may be generalized to include arrangements where different coatings are used for the upper and lower guide walls surrounding the deflector plate. Indeed if one of the walls is deemed to have 100% reflectivity at all angles the net result is an arrangement that, by symmetry, is identical in behavior to that of a V-shaped polarizing cavity [22]. In the future we intend to investigate the transmission properties of single and double V-shaped cavities using an extension of the formalism described in this paper.

Acknowledgements

Many thanks to David Mildner, Chuck Majkrzak, and Jeremy Cook for several helpful discussions, and to Yiming Qiu for considerable help with the figures. I am also grateful to Anna Sokolova, Peter Böni, and Phillip Bentley, for their interest in this work.

Appendix. Basic operations on acceptance diagram polygons

In the present context there are 3 basic operations on acceptance diagram polygons.

(i) The *split* operation is used to separate the neutrons according to the surface that they will next encounter. This is achieved by separating the polygon into 2 smaller polygons, below and above the corresponding horizontal line (constant y).
(ii) The *chop* operation distinguishes between neutrons reflected and transmitted by a reflective surface. In this case the starting polygon is separated into 2 smaller polygons either side of the corresponding vertical line (constant β).
(iii) The *rotate* operation, representing the transformation that occurs on reflection, involves rotation through 180° about a specified point.

We now discuss the various operations that are performed on polygons representing neutrons at the entrance and in the upper and lower cavities of the deflector section.

Neutrons entering the deflector section (state I): the polygon is split at $y=W$. The upper polygon represents neutrons approaching the upper guide surface (state U). The lower polygon represents neutrons approaching the deflector surface from above (state L).

Neutrons in the upper cavity, approaching the upper guide surface (states U, H, and T): the polygon is chopped at $\beta=\theta_0$. The left-hand polygon, with $\beta<\theta_0$, is rotated about the point (0,W); it represents reflected neutrons in state G. The right-hand polygon, with $\beta>\theta_0$, represents transmitted neutrons in state A.

Neutrons in the upper cavity, approaching the deflector surface from above (states L and G): the polygon is chopped at $\beta=-\theta_\alpha+\alpha$. The right-hand polygon, representing reflected neutrons in state H, with $\beta>-\theta_\alpha+\alpha$, is rotated about the point (α,W). The left-hand polygon, with $\beta<-\theta_\alpha+\alpha$, represents transmitted neutrons in state S.

Neutrons in the lower cavity, approaching the lower guide surface or the guide exit (states J and S): the polygon is split at $y=-W$. The upper polygon represents neutrons that escape in state C. The lower polygon is chopped at $\beta=-\theta_0$. The lower right-hand polygon, with $\beta>-\theta_0$, is rotated about the point (0,−W); it represents reflected neutrons in state K. The lower left-hand polygon, with $\beta<-\theta_0$, represents transmitted neutrons in state E.

Neutrons in the lower cavity, approaching the deflector surface from below or the guide exit (state K): the polygon is split at $y=W$. The upper polygon is then chopped at $\beta=\theta_\alpha+\alpha$. The upper left-hand polygon, with $\beta<\theta_\alpha+\alpha$, is rotated about the point (α,W);

it represents reflected neutrons in state J. The upper right-hand polygon, with $\beta > \theta_\alpha + \alpha$, represents transmitted neutrons in state T. The lower polygon represents neutrons that escape in state C.

References

[1] J.M. Carpenter, D.F.R. Mildner, Nucl. Instr. and Meth 196 (1982) 341.
[2] I.S. Anderson, Proc. SPIE 983 (1989) 84.
[3] J.R.D. Copley, Nucl. Instr. and Meth. A 287 (1990) 363.
[4] J.R.D. Copley, J. Neut. Res 1 (1993) 21.
[5] D.F.R. Mildner, Nucl. Instr. and Meth 200 (1982) 167.
[6] D.F.R. Mildner, Nucl. Instr. and Meth. A 301 (1991) 395.
[7] D.F.R. Mildner, Nucl. Instr. and Meth. A 290 (1990) 189.
[8] J.R.D. Copley, D.F.R. Mildner, Nucl. Sci. Eng 110 (1992) 1.
[9] D.F.R. Mildner, J.C. Cook, Nucl. Instr. and Meth. A 592 (2008) 414.
[10] J.B. Hayter, Proc. SPIE 1738 (1992) 2.
[11] J.R.D. Copley, J. Neut. Res 2 (1994) 95.
[12] F. Mezei, Proc. SPIE 983 (1989) 10.
[13] J.R.D. Copley, Nucl. Instr. and Meth. A 301 (1991) 191.
[14] J.R.D. Copley, Nucl. Instr. and Meth. A 332 (1993) 511.
[15] J.R.D. Copley, Nucl. Instr. and Meth. A 510 (2003) 318.
[16] J.M. Carpenter, D.F.R. Mildner, Nucl. Instr. and Meth. A 301 (1991) 315.
[17] J.M. Carpenter, D.F.R. Mildner, Nucl. Instr. and Meth. A 325 (1993) 255.
[18] J.R.D. Copley, C.F. Majkrzak, Proc. SPIE 983 (1989) 93.
[19] For a listing of L.D. Cussen's publications go to ⟨http://cussenconsulting.com/index.html⟩.
[20] P.M. Bentley, K.H. Andersen, Nucl. Instr. and Meth. A 602 (2009) 564.
[21] Paul E. Black, Level-order traversal, in: Dictionary of Algorithms and Data Structures [online], Paul E. Black (Ed.), US National Institute of Standards and Technology, 6 October 2010, (accessed 15 February 2011) available from: ⟨http://xw2k.nist.gov/dads/HTML/levelOrderTraversal.html⟩.
[22] P. Böni, W. Münzer, A. Ostermann, Physica B 404 (2009) 2620.